ACS APPLIED MATERIALS & INTERFACES

Research Article

www.acsami.org

Novel Carbazol-Pyridine-Carbonitrile Derivative as Excellent Blue Thermally Activated Delayed Fluorescence Emitter for Highly Efficient Organic Light-Emitting Devices

Wei Liu,[†,‡] Cai-Jun Zheng,[*,†] Kai Wang,[†,§] Zhan Chen,[†,§] Dong-Yang Chen,[†,§] Fan Li,[†] Xue-Mei Ou,[†] Yu-Ping Dong,[*,‡] and Xiao-Hong Zhang[*,†,∥]

[†]Nano-organic Photoelectronic Laboratory and Key Laboratory of Photochemical Conversion and Optoelectronic Materials, Technical Institute of Physics and Chemistry, Chinese Academy of Sciences, Beijing 100190, P. R. China

[‡]College of Materials Science and Engineering, Beijing Institute of Technology, Beijing 100081, P. R. China

[§]University of the Chinese Academy of Sciences, Beijing 100039, P. R. China

[∥]Functional Nano & Soft Materials Laboratory (FUNSOM) and Collaborative Innovation Center of Suzhou Nano Science and Technology, Soochow University, Suzhou, Jiangsu 215123, P.R. China

Supporting Information

ABSTRACT: A novel blue thermally activated delayed fluorescence (TADF) emitter, CPC (2,6-di(9*H*-carbazol-9-yl)-4-phenylpyridine-3,5-dicarbonitrile), was designed and synthesized. By directly linking carbazole (to serve as electron-donor) and pyridine-3,5-dicarbonitrile (to serve as electron-acceptor), and distributing cyanogroups and carbazole groups at the para-position of pyridine core, CPC successfully achieves an extremely small singlet−triplet splitting and fairish photoluminescence quantum yield, thus can act as the highly efficient blue TADF emitter. The optimized organic light-emitting diode (OLED) based on 13 wt % CPC doped in mCP (1,3-bis(9*H*-carbazol-9-yl)benzene) host exhibits maximum current efficiency, power efficiency, and external quantum efficiency of 47.7 cd A^{-1}, 42.8 lm W^{-1}, and 21.2%, respectively, which are the best results in reported blue TADF-based devices up to date and even comparable with the best reported blue phosphorescent OLEDs.

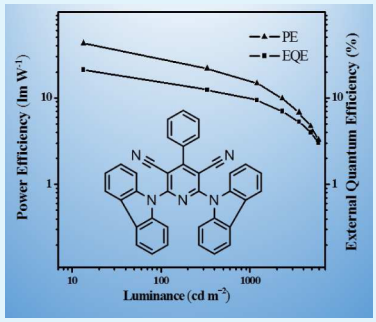

KEYWORDS: *TADF, charge transfer transition, carbazole, pyridine, carbonitrile, blue emitter, OLEDs*

1. INTRODUCTION

Organic light-emitting diodes (OLEDs) have attracted great interest for their applications in large-area, high-resolution flat panel displays and full-color lighting sources.[1−3] In devices, electrically injected charge carriers recombine to form singlet and triplet excitons in a 1:3 ratio. Electroluminescence (EL) internal quantum efficiencies (IQE) of conventional fluorescent materials are limited to 25% because of only singlet excitons can be harvested for lighting in devices. Meanwhile, noble-metal-based organometallic phosphorescent emitters can theoretically harvest both singlet and triplet excitons, realizing 100% IQE; but their further development is hindered due to high cost of noble metals and poor stability of blue phosphors. As an alternative, thermally activated delayed fluorescence (TADF) based on conventional organic aromatic fluorophors, which can also achieve fully excitions utilization through efficient upconversion of nonradiative triplets to radiative singlets, has drawn great attention in recent two years.[4−11] Actually, highly efficient TADF-based green OLEDs with external quantum efficiencies (EQEs) of 19.3%[4] or even higher[12,13] have been successfully realized, proving theoretical 100% IQE of TADF mechanism. Therefore, TADF-based OLEDs have been considered as the new generation OLEDs.

For practical applications in full-color displays and lightings, three primary colors, red, green, and blue, are basically required. Especially, high performance blue emission is rather crucial to reduce the power consumption of a full-color OLEDs. Moreover, high performance blue TADF-based devices can precisely solve the bottleneck of blue phosphorescent OLEDs. Thus, it is more urgent to develop high performance blue TADF emitters. However, efficient blue TADF emitters have scarcely been reported. In 2012, Adachi and co-workers have reported blue TADF emitters 2CzIPN and bis[4-(3,6-di-*tert*-butylcarbazole)phenyl]sulfone with low EQEs of 8.0% and 9.9%, respectively.[4,14] Likewise, Lee and co-workers designed BFCz-2CN which had an improved EQE of 12.1% and efficiency roll-off.[15] Though recently a highly efficient blue TADF-based OLED with EQE of 19.5% was fabricated by using DMAC-DPS as the emitter,[16] it is still a challenge to achieve high performance blue TADF emitters with extremely small singlet−triplet splitting (ΔE_{ST}) and high photoluminescence quantum yield (PLQY) simultaneously.[17]

Received: June 25, 2015
Accepted: August 20, 2015
Published: August 20, 2015

ACS Publications © 2015 American Chemical Society

DOI: 10.1021/acsami.5b05648
ACS Appl. Mater. Interfaces 2015, 7, 18930−18936

In this work, we designed and synthesized a novel blue TADF emitter 2,6-di(9*H*-carbazol-9-yl)-4-phenylpyridine-3,5-dicarbonitrile (CPC) for highly efficient OLEDs. Generally, improving separation of the highest occupied molecular orbital (HOMO) and lowest unoccupied molecular orbital (LUMO) in a single molecule results in a small ΔE_{ST}, but it is usually not beneficial for effective charge transfer (CT) transition. Therefore, it is essential for high performance TADF emitters to keep a precise separation of HOMO and LUMO to get a small ΔE_{ST} and efficient CT emission simultaneously. As shown in Scheme 1, the pyridine-3,5-dicarbonitrile electron-acceptor (A) and carbazole electron-donor (D), which are reported to have outstanding carrier-transporting property and high electrochemical stability,[18−24] are linked directly to form CPC molecule. Such direct linking induces a large twist between D and A segments, thus producing small overlap between HOMO and LUMO, which contributes to a small ΔE_{ST}. And cyano groups and carbazole groups located at the para-position of pyridine core can benefit CT transition, leading to fairish PLQY from intramolecular CT excitons.[25] The rational designed CPC successfully shows highly efficient blue TADF, and the OLEDs based on CPC exhibits maximum current efficiency (CE), power efficiency (PE) and EQE of 47.7 cd A^{-1}, 42.8 lm W^{-1}, and 21.2%, respectively, which is the highest efficiency of blue TADF-based OLEDs up to date and even comparable with the best reported phosphorescent devices.[26−28] These results indicate that CPC is an excellent blue TADF emitter for highly efficient OLEDs.

Scheme 1. Synthetic Route and Molecular Structure of CPC

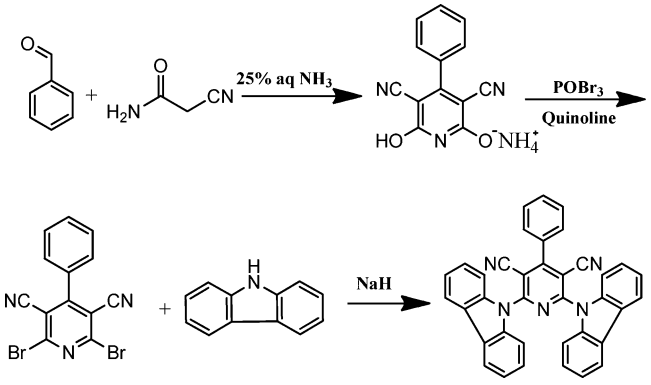

2. RESULTS AND DISCUSSION

2.1. Synthesis. Scheme 1 illustrates the synthetic route and molecular structure of CPC. Ammonium 3,5-dicyano-6-hydroxy-4-phenylpyridin-2-olate was first synthesized using cyanocetamide and benzaldehyde through a cyclization reaction. Then, the resulting ammonium 3,5-dicyano-6-hydroxy-4-phenylpyridin-2-olate went through a halogenating reaction by phosphorus oxybromide giving the next intermediate 2,6-dibromo-4-phenylpyridine-3,5-dicarbonitrile. Finally, CPC was synthesized via the NaH-assisted cross-coupling reaction between 2,6-dibromo-4-phenylpyridine-3,5-dicarbonitrile and carbazole. The chemical structure was fully characterized and confirmed via nuclear magnetic resonance (NMR) spectroscopy and mass spectrometry (MS). Moreover, the compound was further purified by sublimation before it was used for fabricating devices.

2.2. Photophysical Properties. Room-temperature ultraviolet−visible (UV−vis) absorption of CPC in toluene, fluorescence and phosphorescence spectra of 13 wt % CPC doped 1,3-bis(9H-carbazol-9-yl)benzene (mCP) film at 77K are shown in Figure 1a. In toluene, the first absorption peak at 283 nm is assigned to the carbazole centered $n-\pi^*$ transition, while the strong absorption peak at 374 nm is attributed to the CT transition from the electron-rich carbazole moiety to the electron-deficient pyridine-3,5-dicarbonitrile group. Such strong CT absorption has seldom been observed in conventional TADF compounds due to the small overlap between HOMO and LOMO. And in CPC, it should be attributed to the para-substitutions of cyanogroups and carbazole groups on pyridine core, and the strong electron-withdraw ability of pyridine-3,5-dicarbonitrile group and strong electron-donate ability of carbazole groups. Based on the fluorescence and phosphorescence spectra of CPC doped mCP film at 77 K, ΔE_{ST} is determined to be 0.04 eV by the difference between the onset of the fluorescence spectrum (448 nm, S_1 = 2.77 eV) and that of the phosphorescence spectrum (455 nm, T_1 = 2.73 eV). Moreover, CPC shows a blue emission in toluene solution with a peak at 474 nm (Figure 1b), which is attributed to the ICT transition. To prove that CPC undergoes an ICT transition, we measured the PL spectra of CPC in a series of solvents with different polarities (Figure 1b). CPC displays strong solvatochromaticity such that the emission spectrum exhibits a clear bathochromic shift from low polar toluene to higher polar ethyl acetate, dichloromethane (DCM) and dimethylformamide (DMF).[29] The PLQY of 13 wt % CPC doped mCP

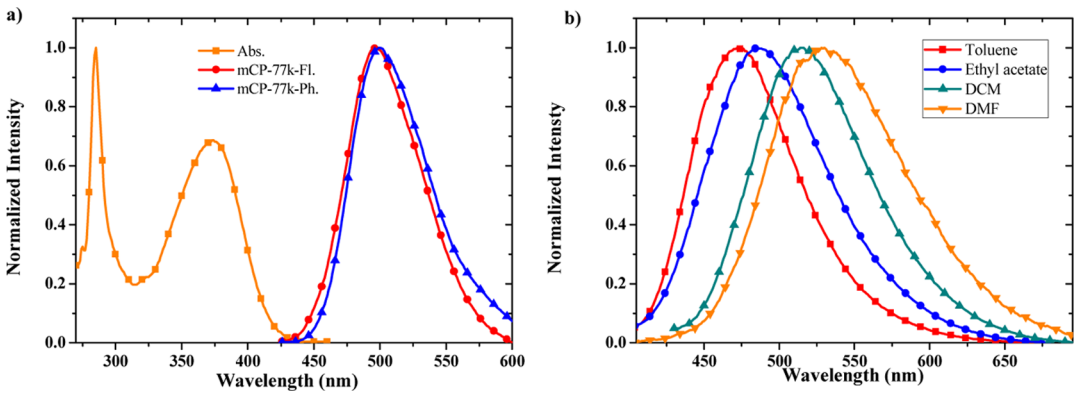

Figure 1. (a) Room-temperature UV−vis absorption spectrum in toluene and fluorescence and phosphorescence spectra of 13 wt % CPC doped mCP film at 77 K. (b) PL spectra of CPC in different solvents at room temperature.

DOI: 10.1021/acsami.5b05648
ACS Appl. Mater. Interfaces 2015, 7, 18930−18936

film in ambient atmosphere was determined to be 49.7% (obtained via integrating sphere measurements). The small ΔE_{ST} and high PLQY in doped film of CPC suggested that it would be a promising candidate as high performance blue TADF emitter.

To further prove the TADF property of CPC, the transient decay characteristics of 13 wt % CPC doped mCP film were measured in ambient atmosphere. Mixed film exhibits a prompt decay with a lifetime of 9.7 ns in the time range of 100 ns (Figure S1), and a delayed decay with a lifetime of 46.6 μs in the time range of 350 μs at room temperature. With the increased temperatures, the delayed decays of CPC doped mCP film become more significant as shown in Figure 2,

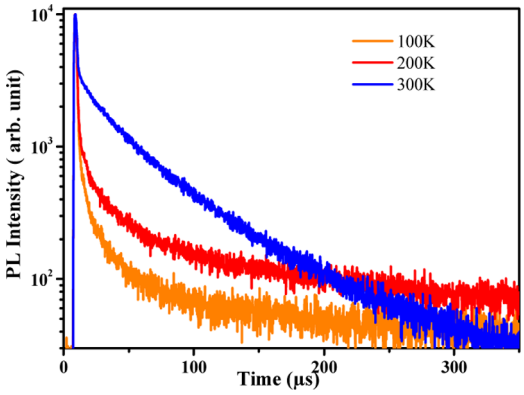

Figure 2. Transient PL decay curve for delayed emission of 13 wt % CPC doped mCP film in time range of 350 μs. (Excitation wavelength was 300 nm.)

proving that reverse intersystem crossing (RISC) process from T_1 state to S_1 state of CPC is remarkably enhanced by the increased temperatures, which is the direct evidence for TADF emitters.

2.3. Theoretical Calculations and Electrochemical Properties. To gain insight into the structure−property relationship of the compound at the molecular level, density functional theory (DFT) based calculations were performed for CPC as shown in Figure 3. The molecule shows a symmetrical

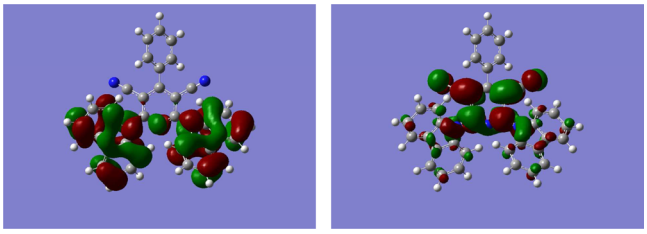

Figure 3. Calculated spatial distributions of the HOMO (left) and LUMO (right) of CPC.

twisted structure which is essential for separating HOMO and LUMO distribution effectively. The dihedral angle between the planes of carbazole group and pyridine core is 48.5°, and it is larger a bit (51.4°) for benzene and the pyridine group. Interestingly, the cyanogroups do not share the same plane with the pyridine core, and this also suggests CPC is highly twisted and rigid. Thus, the HOMO of CPC is primarily confined at the two carbazole units because of the strong electron-donating ability of the carbazole units. And the electron distributions of LUMO are mostly located at the electron-deficient carbonitrile moiety and the pyridine-core. The overlap between HOMO and LUMO is extremely small for CPC, ensuring the small ΔE_{ST} of the molecule. Meanwhile, the slight HOMO−LUMO overlap also ensures fairish radiative decay from intramolecular CT excitons. Moreover, large steric hindrances of carbazole groups, cyano groups, and benzene groups substituted on pyridine core lead to a rigid structure of CPC compound, which can limit torsional flexibility, thus preventing nonradiative transition.[4] All of these results ensure that CPC becomes a promising TADF emitter for high performance OLEDs.

Cyclic voltammetry was used to investigate the electrochemical properties of CPC. As shown in Figure S2, the values of HOMO and LUMO energy levels were determined to be −6.25 and −3.47 eV from the onset of its oxidation/reduction potential with respect to that of ferrocene, respectively. Based on the CV results, the energy gap of CPC is estimated to be 2.78 eV, which is consistent with the result estimated from the onset of the fluorescence spectrum of CPC doped mCP film at 77 K.

2.4. Thermal Properties. Thermal properties of CPC were determined by thermogravimetric analysis (TGA) and differential scanning calorimetry (DSC) under a nitrogen atmosphere (Figure S3). The decomposition temperature (T_d, corresponding to 5% weight loss) of CPC is as high as 350 °C, and glass transition is not observed from 50 to 300 °C. Such results are beneficial to the morphological stability of the film, and expected to decrease the phase separation rate of the guest−host system.

2.5. Electroluminescence Performance. Based on the unique characteristics of CPC, TADF-based OLEDs with different CPC doping concentrations in mCP as the emitting layers (EML) were first fabricated with an optimized structure of ITO/TAPC (40 nm)/TCTA (5 nm)/EML (20 nm)/TmPyPB (40 nm)/LiF (0.8 nm)/Al. In these devices, ITO (indium tinoxide) and LiF/Al (lithium fluoride/aluminum) are the anode and the cathode, respectively; TAPC (4,4′-cyclohexylidenebis[*N*,*N*-bis(4-methylphenyl)aniline]) is the hole-transporting layer. TCTA (4,4′,4″-tris(*N*-carbazolyl)-triphenylamine) is the exciton-blocking layer. TmPyPB (1,3,5-tri[(3,2-pyridyl)-phen-3-yl]benzene) is the electron-transporting, hole-blocking, and exciton-blocking layer.

As listed in Table 1, the maximum EQEs of devices are enlarged along with the increase of doping concentration from 9.8% at 5 wt % to a maximum of 21.2% at 13 wt %, which is mainly attributed to the more efficient exciton utilization with higher emitter component; while decreased with the further concentration increase due to the strong interaction and aggregation between CPC molecules at high doping concentration in the EML.[30,31] As shown in Figure S4, all the devices exhibit stable blue emissions at different luminances. With the increase of doping concentration from 5 to 50 wt %, the EL spectra red-shifted from sky-blue emission with a maximum wavelength of 475 nm and a CIE coordinate of (0.18, 0.26) to greenish-blue emission with a maximum wavelength of 510 nm and a CIE coordinate of (0.24, 0.40) (Figure 4). On the one hand, such red-shift is probably caused by the interaction between CPC molecules; on the other hand, the CPC molecules can also increase the polarity of the EML thus introducing solvatochromaticity like in solutions.[32,33] The turn on voltages (at a brightness of 1 cd m^{-2}) are lowered from 3.4 V at 5 wt % to 3.1 V at 30 wt %, mainly due to the charge trapping effect of CPC dopant. Interestingly, the efficiency roll-off of 50 wt % doping concentration device is smaller than that

DOI: 10.1021/acsami.5b05648
ACS Appl. Mater. Interfaces 2015, 7, 18930−18936

Table 1. Summary of CPC-Based OLEDs Performance

host	doping conccn (wt %)	V_{on} (V)[a]	EL_{max} (nm)[b]	EQE_{max} (%)[c]	EQE (%) at 50 cd m^{-2}	EQE (%) at 500 cd m^{-2}	efficiency roll-off (%)[d]	CIE (x, y) at 500 cd m^{-2}
mCP	5	3.4	475	9.8	8.4	5.7	32	(0.18, 0.26)
mCP	7	3.4	477	13.8	10.9	7.4	32	(0.18, 0.29)
mCP	9	3.3	479	15.3	11.4	7.8	32	(0.19, 0.31)
mCP	11	3.2	485	18.7	14.7	9.9	32	(0.19, 0.32)
mCP	13	3.2	490	21.2	17.0	11.3	33	(0.20, 0.35)
mCP	15	3.2	495	15.7	14.4	10.8	25	(0.21, 0.38)
mCP	30	3.1	508	11.5	10.1	7.8	23	(0.23, 0.39)
mCP	50	3.1	510	8.0	7.4	6.3	15	(0.24,0.40)
DPEPO[e]	15	4.6	474	11.7	8.5	3.4	60	(0.18, 0.26)
26DCZPPY[e]	10	3.1	512	15.5	12.5	8.8	30	(0.23, 0.39)

[a]Turn-on voltage, estimated at the brightness of 1 cd m^{-2}. [b]Maximum wavelength of EL. [c]External quantum efficiency. [d]The roll-off efficiency from the brightness of 50−500 cd m^{-2} [e]Device performance of the host DPEPO/26DCZPPY with the optimized structures.

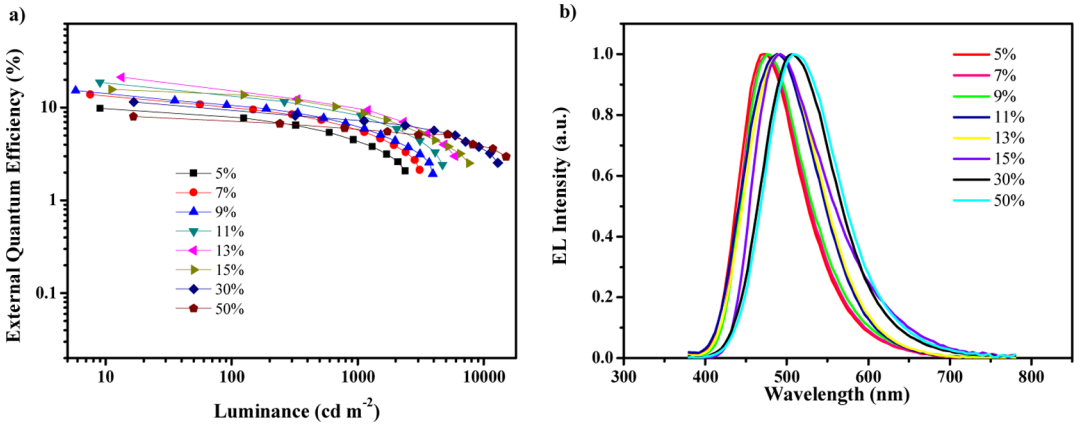

Figure 4. (a) Luminance−EQE plots and (b) EL spectra of OLEDs based on CPC doped in mCP with different doping concentrations.

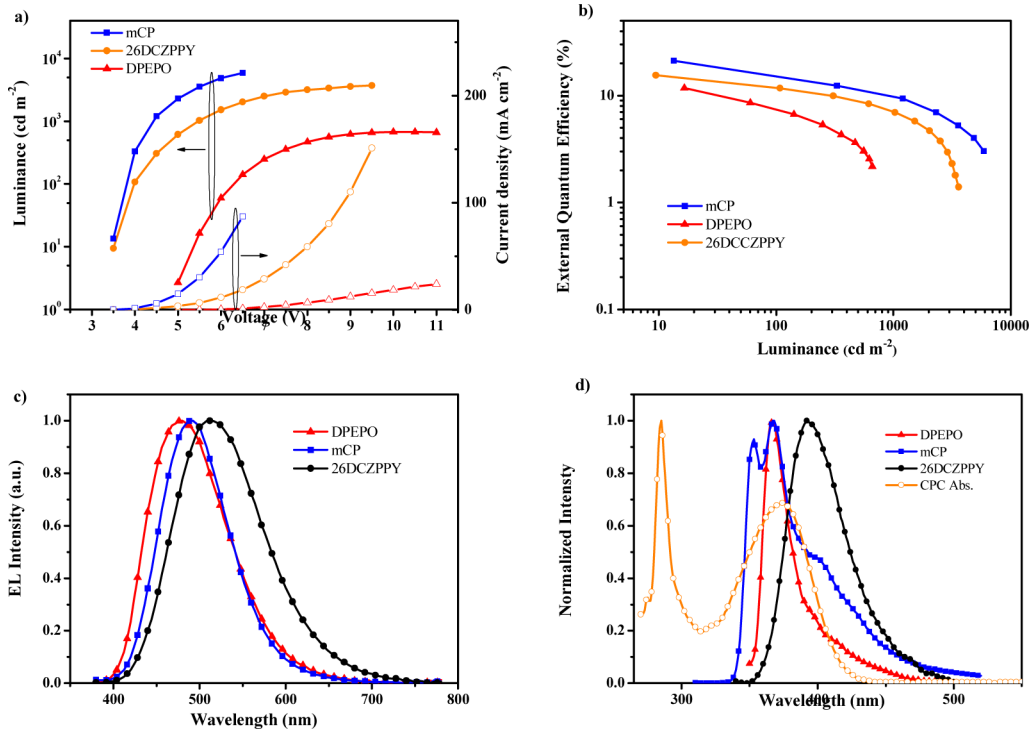

Figure 5. (a) Voltage−luminance−current density characteristics, (b) luminance−EQE plots, (c) EL spectra of OLEDs based on CPC doped in different hosts, and (d) absorption spectrum of CPC and the PL spectra of different hosts.

DOI: 10.1021/acsami.5b05648
ACS Appl. Mater. Interfaces 2015, 7, 18930−18936

of lower doping concentration, which should be caused by two reasons: first, CPC is capable of showing good electron transport property due to the cyanogroups and the pyridine core.[18,19] Therefore, it is thought that recombination zone can move from the interface between EML and ETL to the center of EML which benefits excitons utilization. Second, with the increasing of CPC concentrations, the excitons, especially triplet excitons, can more effectively transfer to the CPC emitters under high current densities which prevent the nonradiation decay and triplet−triplet annihilation on the host.

To further reveal the performance of novel TADF emitter CPC, two more hosts, DPEPO and 26DCZPPY, were chosen to fabricate the devices. CPC was first doped into DPEPO and 26DCZPPY with the same structure of the optimized mCP-based device. As shown in Figure S5 and Table S1, both devices fail to achieve high efficiencies. To obtain the best performance of CPC in those two hosts, the device structures were optimized as ITO/TAPC (30 nm)/TCTA (10 nm)/mCP (10 nm)/15 wt % CPC:DPEPO (10 nm)/DPEPO (10 nm)/TPBI (30 nm)/LiF (0.8 nm)/Al and ITO/TAPC (40 nm)/TCTA (5 nm)/10 wt % CPC:26DCZPPY (10 nm)/TmPyPB (50 nm)/LiF (0.8 nm)/Al, respectively, where TPBI (1,3,5-tri(1-phenyl-1*H*-benzo[*d*]imidazol-2-yl)phenyl) replaces TmPyPB as the electron-transporting layer in DPEPO-based device. With the optimized results of mCP-based device with 13 wt % doping concentration, CPC in three hosts exhibits discriminating EL emissions as shown in Figure 5c. Deepest blue emission with a maximum wavelength of 474 nm and a CIE coordinate of (0.18, 0.26) is obtained by DPEPO host, sky-blue emission with a peak at 490 nm and a CIE coordinate of (0.20, 0.35) by mCP host, and a greenish-blue emission with a maximum wavelength of 512 nm and a CIE coordinate of (0.23, 0.39) by 26DCZPPY host. Red-shifts in the spectra are attributed to increased polarities from DPEPO to mCP and 26DCZPPY.[32,33] Figure 5b shows the EQE versus luminance plots of three optimized devices with different hosts. The device based on DPEPO gives the lowest maximum EQE of 11.7%, which is mainly caused by two reasons. The first is that the poor charge mobility of DPEPO which leads to low carrier utilization.[34] As showed in Figure 5a the maximum current density is only 24 mA cm^{-2}. And another reason is that over high T_1 energy level of DPEPO (3.25 eV) may lead to energy loss in energy transfer from DPEPO host to CPC guest. The OLED based on 26DCZPPY shows a moderate maximum EQE of 15.5%, which is because the poor overlap of absorption spectrum of CPC and the PL spectrum of the 26DCZPPY (Figure 5d) will harm the Förster energy transfer of singlet excitons from 26DCZPPY host to CPC emitter.[35−37] Thus, the best device based on TADF emitter CPC is achieved in mCP host with a 13 wt % doping concentration. The device exhibits a maximum EQE of 21.2%, a maximum CE of 47.7 cd A^{-1}, and a maximum PE of 42.8 lm W^{-1} without any light out-coupling enhancement, indicating nearly 100% excitons harvesting by CPC emitter. Such high performance of the device should be not only attributed to the fairish PLQY of CT emission and efficient RISC process from T_1 to S_1 of CPC emitter, but also owed to the reasonable high T_1, good charge mobility, and well matched PL spectrum of the mCP host with the CPC absorption spectrum. Although, at high current density, the device suffered moderate efficiency roll-off, our device still realized high efficiency, which is the highest result among the reported blue TADF-based devices (Table 2) and even comparable with the best reported phosphorescent devices.

Table 2. Summary of Blue TADF Emitters and OLEDs Performance

emitters	ΔE_{st} (eV)	V_{on} (V)[a]	EL_{max} (nm)[b]	EQE_{max} (%)[c]	CIE (*x*, *y*)
this work[d]	0.04	3.2	490	21.2	(0.20, 0.35)
this work[e]	0.04	4.6	474	11.7	(0.18, 0.26)
ref 2				8.0	
ref 17	0.11		487	20.6	(0.19, 0.35)
ref 4	0.34		423	9.9	(0.15, 0.07)
ref 6	0.08	3.7	470	19.5	(0.16, 0.20)
ref 2	0.05	4.0	462	16.4	(0.17, 0.19)
ref 5	0.13		486	12.1	
ref 2	0.14	4.4	484	14.3	(0.17, 0.27)

[a]Turn-on voltage, estimated at the brightness of 1 cd m^{-2}. [b]Maximum wavelength of EL. [c]External quantum efficiency. [d]The performance of the optimized devices with mCP host. [e]The performance of the optimized device with DPEPO host.

3. CONCLUSION

In summary, we have designed and synthesized a novel efficient blue TADF emitter CPC. By linking carbazole D and pyridine-3,5-dicarbonitrile A segments directly and distributing cyano groups and carbazole groups at the para-position of pyridine core, CPC successfully achieves both extremely small ΔE_{ST} and fairish PLQY, which are essential for highly efficient blue TADF emitter. The OLED based on 13 wt % CPC doped in mCP host exhibits high EQE of 21.2% with a CIE coordinate of (0.20, 0.35). These results are better than other reported blue TADF-based OLEDs and even comparable to that of best blue phosphorescent OLEDs, confirming that our pure organic aromatic TADF fluorophor CPC is promising candidate for achieving low-cost, high-efficiency OLEDs.

4. EXPERIMENTAL SECTION

4.1. General Procedures. NMR spectral data were obtained using a Bruker Advance-400 spectrometer with chemical shifts reported in ppm. Mass spectral data were obtained using a Finnigan 4021C gas chromatography−mass spectrometry instrument. Absorption and photoluminescence spectra were obtained using a Hitachi UV−vis spectrophotometer U-3010 and a Hitachi fluorescence spectrometer F-4600, respectively. The photoluminescence quantum yield of neat solid film was obtained using a QY-2000 fluorescence spectrometer and estimated via an F-3018 integrating sphere. Moreover, DSC measurements were acquired using a NETZSCH DSC204 instrument at a heating rate of 10 °C min^{-1} from 20 to 420 °C in a N_2 atmosphere. TGA measurements were acquired using a TAQ 500 thermogravimeter by measuring the weight loss of the specimens while heating them at a rate of 10 °C min^{-1} from 25 to 800 °C in a N_2 atmosphere. The theoretical calculations of CPC were performed using the Gaussian09 program. DFT B3LPY/6-31G(d) was used to determine and optimize the structures. Transient PL decay characteristics and fluorescence quantum yields were measured with an Edinburgh Instruments FLS920 spectrometer. Cyclic voltammetry was performed on a CHI660E electrochemical analyzer with 0.1 M Bu_4NPF_6 as a supporting electrolyte, a saturated calomel electrode (SCE) as a reference electrode, a Pt disk as a working electrode, and a scan rate of 10 mV/s. The oxidation potential of SCE relative to the vacuum level is calibrated to be 4.60 V in acetonitrile, assuming that the formal potential of the Fc^+/ Fc redox couple is 0.50 V versus SCE in acetonitrile.

4.2. Synthesis. All commercially available reagents and chemicals were used without further purification.

2,6-Dibromo-4-phenylpyridine-3,5-dicarbonitrile. According to the procedure described by Lukes and Kuthan, cyanocetamide (5.98 g, 71.0 mmol) was suspended in H_2O (40 mL), and then 25% aq. NH_3

DOI: 10.1021/acsami.5b05648
ACS Appl. Mater. Interfaces 2015, 7, 18930−18936

(2 mL) and benzaldehyde (3.71 g, 35.0 mmol) were added. The mixture was stirred for 10 h at room temperature. The obtained white precipitate was collected by filtration, washed with small portions of cold MeOH, and dried under reduced pressure to give product ammonium 3,5-dicyano-6-hydroxy-4-phenylpyridin-2-olate (6.22 g, 24.5 mmol, 70%) without further purification. Then phosphorus oxybromide (5.0 g, 8.7 mmol) was added to toluene (30 mL) at room temperature. Next, 3,5-dicyano-6-hydroxy-4-phenylpyridin-2-olate (0.76 g, 3 mmol) and quinoline (3.0 mL) were added consecutively to mechanically stirred reaction mixture to 100 °C. After reaction completion, the toluene layer was separated. The remaining brownish solid was extracted with boiling toluene (3 × 30 mL). The combined toluene solutions were washed with 5% aqueous $NaHCO_3$, dried over anhydrous sodium sulfate, and concentrated by rotary evaporation. Then it was subjected to the silica gel column chromatography (eluent: hexane/CH_2Cl_2 = 1:1) to give 2,6-dibromo-4-phenylpyridine-3,5-dicarbonitrile (0.87 g, 2.4 mmol, 80.1%) as a white solid. ^{1}H NMR (400 MHz, $CDCl_3$, δ) 7.74−7.61 (m, 3H), 7.56 (dd, J = 7.3, 5.8 Hz, 2H). MS (EI) m/z: $[M]^+$ calcd for $C_{13}H_5Br_2N_3$, 362.88; found, 362.8840.

2,6-di(9H-Carbazol-9-yl)-4-phenylpyridine-3,5-dicarbonitrile. According to the synthetic method reported previously for pyrrole and fluorobenzene derivatives,[38] to a tetrahydrofuran (10 mL) solution of NaH (60% oil dispersion, 0.23 g, 5.6 mmol), carbazole (0.84 g, 5 mmol) was added at 0 °C under a nitrogen atmosphere. The reaction mixture was stirred for an additional 30 min at the same temperature, and then a tetrahydrofuran (3 mL) solution of 2,6-dibromo-4-phenylpyridine-3,5-dicarbonitrile (0.73 g, 2.0 mmol) was added. The reaction mixture was stirred for an additional 6 h at room temperature before it was poured into ice-water (40 mL). The yellow precipitate was filtered off and washed with water. Then the mixture was extracted using dichloromethane and distilled water. The dichloromethane phase was dried over Na_2SO_4 and then was filtered. After the solvent was removed under reduced pressure, the crude product was purified through silica gel column chromatography using dichloromethane/methanol (1:1) as an eluant, which produced yellow solid. And further purification was achieved via crystallization with CH_2Cl_2/petroleum ether and sublimation, which produced a yellow-green compound of CPC (0.65 g, 1.2 mmol, 61%). ^{1}H NMR (400 MHz, $CDCl_3$, δ): 8.13 (d, J = 7.4 Hz, 4H), 7.96−7.67 (m, 9H), 7.56−7.36 (m, 8H). ^{13}C NMR (100 MHz, $CDCl_3$, δ): 154.68, 138.77, 132.27, 129.70, 126.81, 125.72, 123.41, 120.71, 113.98, 112.69, 101.13, 77.42, 77.16, 76.84. MS (EI) m/z: $[M]^+$ calcd for $C_{37}H_{21}N_5$, 535.18; found, 535.1804.

4.3. Device Fabrication and Measurement. ITO-coated glasses with a sheet resistance of 30 Ω per square were used as substrates. Before the devices were fabricated, the substrates were first cleaned with acetone, ethanol, and deionized water. Then, they were oven-dried at 120 °C and treated with UV-ozone under ambient conditions for 5 min. Finally, the cleaned glasses were transferred to a vacuum deposition system at approximately 1 × 10^{-6} Torr. Thermally evaporated organic layers were sequentially grown onto the ITO substrates at a rate of 1−2 Å s^{-1}. The cathode was completed via the thermal deposition of LiF at a rate of 0.1 Å s^{-1} and then covered with Al metal deposited at a rate of 10 Å s^{-1}. EL luminances, CIE color coordinates, and spectra were obtained using a Spectrascan PR 650 photometer, and the current−voltage characteristics were determined with a computer-controlled Keithley 2400 SourceMeter in ambient atmosphere. EQE was calculated from the current density, luminance, and EL spectrum, assuming a Lambertian distribution.

■ ASSOCIATED CONTENT

Supporting Information

The Supporting Information is available free of charge on the ACS Publications website at DOI: 10.1021/acsami.5b05648.

Transient PL decay curve of 13 wt % CPC doped mCP film, cyclic voltammograms of CPC, TGA, DSC thermograms of CPC and the normalized EL spectra of the devices at different bias voltage (PDF)

■ AUTHOR INFORMATION

Corresponding Authors

*E-mail: zhengcaijun@mail.ipc.ac.cn.
*E-mail: chdongyp@bit.edu.cn.
*E-mail: xhzhang@mail.ipc.ac.cn.

Notes

The authors declare no competing financial interest.

■ ACKNOWLEDGMENTS

This work was supported by the National Natural Science Foundation of China (Grant No. 51373190), the Beijing Nova Program (Grant No. Z14110001814067), and the Instrument Developing Project of the Chinese Academy of Sciences (Grant No. YE201133), P. R. China.

■ REFERENCES

(1) Reineke, S.; Lindner, F.; Schwartz, G.; Seidler, N.; Walzer, K.; Lüssem, B.; Leo, K. White Organic Light-emitting Diodes with Fluorescent Tube Efficiency. *Nature* **2009**, *459*, 234−238.

(2) Kim, S.; Kwon, H. J.; Lee, S.; Shim, H.; Chun, Y.; Choi, W.; Kwack, J.; Han, D. W.; Song, M.; Kim, S.; Mohammadi, S.; Kee, I. S.; Lee, S. Y. Low-Power Flexible Organic Light-Emitting Diode Display Device. *Adv. Mater.* **2011**, *23*, 3511−3516.

(3) Yu, Z.; Niu, X.; Liu, Z.; Pei, Q. Intrinsically Stretchable Polymer Light-Emitting Devices Using Carbon Nanotube-Polymer Composite Electrodes. *Adv. Mater.* **2011**, *23*, 3989−3994.

(4) Uoyama, H.; Goushi, K.; Shizu, K.; Nomura, H.; Adachi, C. Highly efficient organic light-emitting diodes from delayed fluorescence. *Nature* **2012**, *492*, 234−238.

(5) Mehes, G.; Nomura, H.; Zhang, Q.; Nakagawa, T.; Adachi, C. Enhanced Electroluminescence Efficiency in a Spiro-Acridine Derivative through Thermally Activated Delayed Fluorescence. *Angew. Chem., Int. Ed.* **2012**, *51*, 11311−11315.

(6) Dias, F. B.; Bourdakos, K. N.; Jankus, V.; Moss, K. C.; Kamtekar, K. T.; Bhalla, V.; Santos, J.; Bryce, M. R.; Monkman, A. P. Triplet Harvesting with 100% Efficiency by Way of Thermally Activated Delayed Fluorescence in Charge Transfer OLED Emitters. *Adv. Mater.* **2013**, *25*, 3707−3714.

(7) Wang, H.; Xie, L.; Peng, Q.; Meng, L.; Wang, Y.; Yi, Y.; Wang, P. Novel Thermally Activated Delayed Fluorescence Materials-Thioxanthone Derivatives and Their Applications for Highly Efficient OLEDs. *Adv. Mater.* **2014**, *26*, 5198−5204.

(8) Tao, Y.; Yuan, K.; Chen, T.; Xu, P.; Li, H.; Chen, R.; Zheng, C.; Zhang, L.; Huang, W. Thermally Activated Delayed Fluorescence Materials Towards the Breakthrough of Organoelectronics. *Adv. Mater.* **2014**, *26*, 7931−7958.

(9) Leitl, M. J.; Krylova, V. A.; Djurovich, P. I.; Thompson, M. E.; Yersin, H. Phosphorescence versus Thermally Activated Delayed Fluorescence. Controlling Singlet-Triplet Splitting in Brightly Emitting and Sublimable Cu(I) Compounds. *J. Am. Chem. Soc.* **2014**, *136*, 16032−16038.

(10) Cho, Y. J.; Yook, K. S.; Lee, J. Y. Cool and Warm Hybrid White Organic Light-emitting Diode with Blue Delayed Fluorescent Emitter both as Blue Emitter and Triplet Host. *Sci. Rep.* **2015**, *5*, 7859−7864.

(11) Lee, S. Y.; Yasuda, T.; Yang, Y. S.; Zhang, Q. S.; Adachi, C. Luminous Butterflies: Efficient Exciton Harvesting by Benzophenone Derivatives for Full-Color Delayed Fluorescence OLEDs. *Angew. Chem.* **2014**, *126*, 6520.

(12) Sun, J. W.; Lee, J. H.; Moon, C. K.; Kim, K. H.; Shin, H.; Kim, J. J. A Fluorescent Organic Light-Emitting Diode with 30% External Quantum Efficiency. *Adv. Mater.* **2014**, *26*, 5684−5688.

(13) Lee, D. R.; Kim, B. S.; Lee, C. W.; Im, Y.; Yook, K. S.; Hwang, S. H.; Lee, J. Y. Above 30% External Quantum Efficiency in Green Delayed Fluorescent Organic Light-Emitting Diodes. *ACS Appl. Mater. Interfaces* **2015**, *7*, 9625−9629.

(14) Zhang, Q.; Li, J.; Shizu, K.; Huang, S.; Hirata, S.; Miyazaki, H.; Adachi, C. Design of Efficient Thermally Activated Delayed

DOI: 10.1021/acsami.5b05648
ACS Appl. Mater. Interfaces 2015, 7, 18930−18936

Fluorescence Materials for Pure Blue Organic Light Emitting Diodes. *J. Am. Chem. Soc.* **2012**, *134*, 14706−14709.
(15) Lee, D. R.; Hwang, S. H.; Jeon, S. K.; Lee, C. W.; Lee, J. Y. Benzofurocarbazole and Benzothienocarbazole as Donors for Improved Quantum Efficiency in Blue Thermally Activated Delayed Fluorescent Devices. *Chem. Commun.* **2015**, *51*, 8105−8107.
(16) Zhang, Q.; Li, B.; Huang, S.; Nomura, H.; Tanaka, H.; Adachi, C. Efficient Blue Organic Light-Emitting Diodes Employing Thermally Activated Delayed Fluorescence. *Nat. Photonics* **2014**, *8*, 326−332.
(17) Hirata, S.; Sakai, Y.; Masui, K.; Tanaka, H.; Lee, S. Y.; Nomura, H.; Nakamura, N.; Yasumatsu, M.; Nakanotani, H.; Zhang, Q.; Shizu, K.; Miyazaki, H.; Adachi, C. Highly Efficient Blue Electroluminescence Based on Thermally Activated Delayed Fluorescence. *Nat. Mater.* **2015**, *14*, 330−336.
(18) Li, N.; Wang, P.; Lai, S. L.; Liu, W.; Lee, C. S.; Lee, S. T.; Liu, Z. Synthesis of Multiaryl-Substituted Pyridine Derivatives and Applications in Non-doped Deep-Blue OLEDs as Electron-Transporting Layer with High Hole-Blocking Ability. *Adv. Mater.* **2010**, *22*, 527−530.
(19) You, J.; Lai, S. L.; Liu, W.; Ng, T. W.; Wang, P.; Lee, C. S. Bipolar Cyano-Substituted Pyridine Derivatives for Applications in Organic Light-Emitting Devices. *J. Mater. Chem.* **2012**, *22*, 8922−8929.
(20) Wong, W. Y.; Ho, C. L.; Gao, Z. Q.; Mi, B. X.; Chen, C. H.; Cheah, K. W.; Lin, Z. Multifunctional Iridium Complexes Based on Carbazole Modules as Highly Efficient Electrophosphors. *Angew. Chem., Int. Ed.* **2006**, *45*, 7800−7803.
(21) Mondal, E.; Hung, W. Y.; Dai, H. C.; Wong, K. T. Fluorene-Based Asymmetric Bipolar Universal Hosts for White Organic Light Emitting Devices. *Adv. Funct. Mater.* **2013**, *23*, 3096−3105.
(22) Mondal, E.; Hung, W. Y.; Chen, Y. H.; Cheng, M. H.; Wong, K. T. Molecular Topology Tuning of Bipolar Host Materials Composed of Fluorene-Bridged Benzimidazole and Carbazole for Highly Efficient Electrophosphorescence. *Chem. - Eur. J.* **2013**, *19*, 10563−10572.
(23) Duan, L.; Qiao, J.; Sun, Y. D.; Qiu, Y. Strategies to Design Bipolar Small Molecules for OLEDs: Donor-Acceptor Structure and Non-Donor-Acceptor Structure. *Adv. Mater.* **2011**, *23*, 1137−1144.
(24) Hung, W. Y.; Chi, L. C.; Chen, W. J.; Mondal, E.; Chou, S. H.; Wong, K. T.; Chi, Y. A Carbazole−Phenylbenzimidazole Hybrid Bipolar Universal Host for High Efficiency RGB and White Pholeds with High Chromatic Stability. *J. Mater. Chem.* **2011**, *21*, 19249−19256.
(25) Li, W.; Liu, D.; Shen, F.; Ma, D.; Wang, Z.; Feng, T.; Xu, Y.; Yang, B.; Ma, Y. A Twisting Donor-Acceptor Molecule With an Intercrossed Excited State for Highly Efficient, Deep-Blue Electroluminescence. *Adv. Funct. Mater.* **2012**, *22*, 2797−2803.
(26) Udagawa, K.; Sasabe, H.; Cai, C.; Kido, J. Low-Driving-Voltage Blue Phosphorescent Organic Light-Emitting Devices with External Quantum Efficiency of 30%. *Adv. Mater.* **2014**, *26*, 5062−5066.
(27) Hang, X. C.; Fleetham, T.; Turner, E.; Brooks, J.; Li, J. Highly Efficient Blue-Emitting Cyclometalated Platinum (II) Complexes by Judicious Molecular Design. *Angew. Chem., Int. Ed.* **2013**, *52*, 6753−6756.
(28) Shin, H.; Lee, S.; Kim, K. H.; Moon, C. K.; Yoo, S. J.; Lee, J. H.; Kim, J. J. Blue Phosphorescent Organic Light-Emitting Diodes Using an Exciplex Forming Co-host with the External Quantum Efficiency of Theoretical Limit. *Adv. Mater.* **2014**, *26*, 4730−4734.
(29) Zheng, M.; Bai, F. L.; Zhu, D. B. Intra- and Intermolecular Charge-transfer Phenomena in a Triphenylamine-containing Anthrylenevinylene-based Copolymer and its Model Compound. *Polym. Adv. Technol.* **2003**, *14*, 292−296.
(30) Zhang, Y.; Forrest, S. R. Triplets Contribute to Both an Increase and Loss in Fluorescent Yield in Organic Light Emitting Diodes. *Phys. Rev. Lett.* **2012**, *108*, 267404−267409.
(31) Adachi, C.; Baldo, M. A.; Forrest, S. R. Electroluminescence Mechanisms in Organic Light Emitting Devices Employing A Europium Chelate Doped in A Wide Energy Gap Bipolar Conducting Host. *J. Appl. Phys.* **2000**, *87*, 8049−8052.
(32) Chang, W.; Congreve, D. N.; Hontz, E.; Bahlke, M. E.; McMahon, D. P.; Reineke, S.; Wu, T. C.; Bulovic, V.; Van Voorhis, T.; Baldo, M. A. Spin-dependent charge transfer state design rules in organic photovoltaics. *Nat. Commun.* **2015**, *6*, 6415.
(33) Madigan, C. F.; Bulovic, V. Solid State Solvation in Amorphous Organic Thin Films. *Phys. Rev. Lett.* **2003**, *91*, 247403−247412.
(34) Han, C. M.; Zhao, Y. B.; Xu, H.; Chen, J. S.; Deng, Z. P.; Ma, D. G.; Li, Q.; Yan, P. F. A Simple Phosphine−Oxide Host with a Multi-insulating Structure: High Triplet Energy Level for Efficient Blue Electrophosphorescence. *Chem. - Eur. J.* **2011**, *17*, 5800−5803.
(35) Nakanotani, H.; Higuchi, T.; Furukawa, T.; Masui, K.; Morimoto, K.; Numata, M.; Tanaka, H.; Sagara, Y.; Yasuda, T.; Adachi, C. High-efficiency organic light-emitting diodes with fluorescent emitters. *Nat. Commun.* **2014**, *5*, 4016−4021.
(36) Zhang, D.; Duan, L.; Li, C.; Li, Y.; Li, H.; Zhang, D.; Qiu, Y. High-Efficiency Fluorescent Organic Light-Emitting Devices Using Sensitizing Hosts with a Small Singlet−Triplet Exchange Energy. *Adv. Mater.* **2014**, *26*, 5050−5055.
(37) Higuchi, T.; Nakanotani, H.; Adachi, C. High-Efficiency White Organic Light-Emitting Diodes Based on a Blue Thermally Activated Delayed Fluorescent Emitter Combined with Green and Red Fluorescent Emitters. *Adv. Mater.* **2015**, *27*, 2019−2023.
(38) UNO, H.; Takiue, T.; Uoyama, H.; Okujima, T.; Yamada, H.; Masuda, G. Preparation Of Highly Conjugated Oligoaza-Pahs Based on The Oxidative Intramolecular Coupling of Bicyclo[2.2.2] Octadiene-Fused Pyrrole. *Heterocycles* **2010**, *82*, 791−802.

DOI: 10.1021/acsami.5b05648
ACS Appl. Mater. Interfaces 2015, 7, 18930−18936